

Fractional-order Modeling of the Arterial Compliance: An Alternative Surrogate Measure of the Arterial Stiffness

Mohamed A. Bahloul and Taous-Meriem Laleg Kirati

Abstract—Recent studies have demonstrated the advantages of fractional-order calculus tools for probing the viscoelastic properties of collagenous tissue, characterizing the arterial blood flow and red cell membrane mechanics, and modeling the aortic valve cusp. In this article, we present novel lumped-parameter equivalent circuit models of the apparent arterial compliance using a fractional-order capacitor (FOC). FOC, which generalizes capacitors and resistors, displays a fractional-order behavior that can capture both elastic and viscous properties through a power-law formulation. The proposed framework describes the dynamic relationship between the blood pressure input and blood volume, using linear fractional-order differential equations. The results show that the proposed models present reasonable fit performance with in-silico data of more than 4,000 subjects. Additionally, strong correlations have been identified between the fractional-order parameter estimates and the central hemodynamic determinants as well as pulse wave velocity indexes. Therefore, fractional-order based paradigm of arterial compliance shows prominent potential as an alternative tool in the analysis of arterial stiffness.

Keywords—Cardiovascular system, Apparent compliance, Input Impedance, Fractional order capacitor, Arterial stiffness

I. INTRODUCTION

OVER the last decades, arterial models have been proven to be extremely useful and effective in unraveling cardiovascular diseases [1], in the medical intervention planning [2], in diseases' treatment and monitoring [3], and in the design and testing of medical devices and simulators [4], [5]. Besides, arterial models have shown great potential in the noninvasive evaluation of physiological parameters, which are not directly accessible, such as the arterial compliance and stiffness [6], [7], [8]. Vascular compliance is defined as the ability of a particular arterial vessel to store blood. It describes the capacitance of the vascular wall to dynamically distend and increase the vessel volume with an increase in the transmural pressure or the tendency of the vascular wall to resist and recoil toward its original geometry with compression. Functionally, arterial compliance is demonstrated by the relationship between the stored blood volume's variation and the input blood pressure's variation. Similarly, the concept of total arterial compliance was introduced as the sum of all compliance components of the entire arterial system. Thus, the total compliance describes the global arterial capacity to store blood and is equal to the variation in blood volume in the entire arterial system divided by the systemic input pressure's variation. However, it is known that this ratio is not only governed by the total arterial compliance but

also incorporates some other effects such as the pulse wave reflection. Indeed, it is equivalent to the total compliance only at low frequency. Hence, the concept of dynamic arterial compliance-or, equivalently, apparent compliance have been proposed by Quick *et al.* [9] to show how to estimate the true total compliance correctly from the transfer function relating the blood volume to the input pressure [10] and explain a question of fact as to whether the classical estimation methods of arterial compliance fails to yield to true arterial compliance. Before the introduction of the "apparent compliance" concept, the transfer function relating blood volume to systemic input pressure is thought to be constant and modeled by a constant capacitance of an ideal capacitor (electrical analog model). This hypothesis is based on the Windkessel concept, which is adopted by the lumped-element modeling school. The drawbacks of this assumption are reflected in its estimation-based methods of compliance, which doesn't yield to a correct evaluation of the true arterial compliance [11]. Because of the distributed nature of the vascular compliance and resistance within the arterial network, the relationship blood Volume/input pressure is frequency-dependent [9]. Accordingly, a time delay between the arterial blood volume and the input pressure occurs. During the past decades, some clinical studies demonstrated the necessity of introducing apparent compliance to extract total compliance. Therefore, a new lumped-parameters modeling framework, which takes into account the complex and frequency-dependence properties of the apparent arterial compliance, have been proposed [12]. These models are based on the idea that the arterial wall is viscoelastic rather than pure elastic. Hence, the Voigt cell model (resistor in series with a capacitor) has been proposed as a suitable candidate to represent the total arterial compliance. The resistor of the Voigt cell displays the viscous losses held by the arterial wall motions, while the capacitor represents the static compliance of the arteries. Through the combination of resistor and capacitor cells gives rise to complex and frequency-dependent compliance, the Voigt model configuration is considered very poor in representing the arterial viscoelasticity properties since it does not account for the *stress-relaxation* experiment [13]. Therefore, to address this inconsistency, the order of the viscoelastic representation has been increased by adding more viscous and elastic connected elements [12]. The higher-order configuration provided a more accurate but complex configuration,

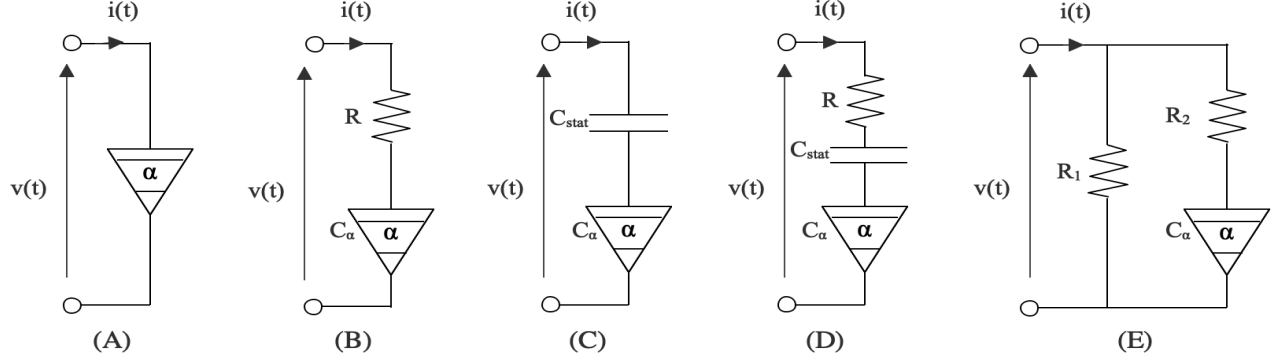


Fig. 1: Schematic representations of the electrical analog of the proposed fractional-order models.

where its complexity is principally due to the enormous number of unknown parameters, which suggests another challenge. Indeed, for higher-order models, the number of parameters to identify is more significant, while the collected real data is small and insufficient. It is also known that reduced-order models are desirable for their simplicity and ease of exploration. Over the last decades, the fractional-order derivative (FD), defined as a generalization of the standard integer derivative to a non-integer order, has been gaining paramount popularity in modeling and characterizing biological tissues [14], [15]. Because of its non-locality and memory properties, FD has been regarded as a powerful tool for modeling complex physical phenomena that exhibit *power-law* response or involve memory effects [16], [17]. In recent research, the power-law behavior has been proved in the viscoelasticity characterization of an elastic aorta. The *in-vivo* and *in-vitro* data analysis showed that the FD tools are more convenient to accurately model and describe the arterial wall viscoelastic dynamic response [18], [19], [20], [21], [22]. Besides, a recent study by the authors [23], [24], used fractional-order derivative tools to the well-known arterial Windkessel paradigm, by replacing the ideal capacitor, which accounts for the total arterial compliance, with a fractional-order capacitor. The preliminary analysis demonstrated that the fractional-order impedance is the right candidate for the accurate assessment of the aortic input impedance. Furthermore, a simple correlation between the main parameters of the central arterial blood pressure and the fractional differentiation operator has been shown. Consequently, the novel fractional-order parameter may have an influential role as a physiological index of the arterial stiffness [25]. This paper introduces and investigates the fractional-order derivative modeling framework for apparent compliance. The proposed modeling framework offers a new paradigm for the physiological interpretation of the frequency-dependent arterial compliance and the interaction between the systemic arterial mechanical properties (viscosity and elasticity). Besides, this study compares the different proposed models as well as with the corresponding integer-order models. The rest of the paper is organized as follows: in Section II, the preliminaries, the proposed models and the method are presented. Section III shows the results and discussion. Finally, section IV presents the conclusion and future perspectives.

II. MATERIAL AND METHOD

A. Preliminaries

1) *Input impedance, apparent compliance, and resistance:* Aortic input impedance (Z_{in}) and apparent compliance (C_{app}) are considered significant in the characterization of the arterial system, independently of the heart properties. Whereas Z_{in} describes the ability of the arterial system to hamper the blood flow dynamically, C_{app} depicts the capacity of the arterial bed to store blood dynamically. Functionally, Z_{in} is defined as the dynamic relationship, in the frequency domain, of the arterial blood pressure (P_{in}) and blood flow (Q_{in}) at the entrance of the systemic circulatory system, that is:

$$Z_{in}(\omega) = \frac{P_{in}(\omega)}{Q_{in}(\omega)}, \quad (1)$$

where ω corresponds to the angular frequency. C_{app} is defined as the dynamic relationship, in the frequency domain, between the blood volume V , and the input aortic blood pressure (P_{in}) that is:

$$C_{app} = \frac{V(\omega)}{P_{in}(\omega)} \quad (2)$$

Similarly, to the concept of apparent compliance, another frequency dependent transfer function relating P_{in} to the output blood flow (Q_{out}) has been defined as well. It describes the so-called apparent resistance (R_{app}) and it can be formulated as:

$$R_{app} = \frac{P_{in}(w)}{Q_{out}(w)} \quad (3)$$

Based on Quik's et al. investigations in [9] and [10], R_{app} can be approximated as a constant that is equivalent to the total peripheral resistance. Additionally, C_{app} can be expressed in terms of Z_{in} and R_{app} :

$$C_{app} = \frac{R_{app} - Z_{in}}{j\omega R_{app} Z_{in}} \quad (4)$$

As mentioned in the previous section, the transfer function describing the apparent compliance is frequency-dependent and describes, not only the total arterial compliance but also incorporates other physiological effects such as pulse reflections. At low frequency, C_{app} converges to a value

that approximates the true total arterial compliance (C_{tot}):

$$C_{tot} = \lim_{w \rightarrow 0} C_{app} \quad (5)$$

2) *Fractional-order capacitor (FOC)*: FOC also known as Constant Phase Element [26], is the main building block for developing analog model structure according to FC. FOC is an electrical element that represents a fractional-order derivative relationship between the current, $i(t)$, passing through and the voltage, $v(t)$, across it with respect to time, t , as follow:

$$i(t) = C_\alpha D_t^\alpha v(t), \quad (6)$$

where C_α is a proportionality constant so-called pseudo-capacitance, expressed in units of [Farad/second $^{1-\alpha}$]. The conventional capacitance, C , in unit of Farad is related to C_α as follow:

$$C = C_\alpha \omega^{\alpha-1}. \quad (7)$$

The impedance (Z_{FOC}) of FOC in Laplace domain is given as:

$$Z_{FOC}(s) = \frac{1}{C_\alpha s^\alpha}. \quad (8)$$

Substituting the *Laplace* variable, s , by $(j\omega)$, (9) can be expressed as:

$$Z_{FOC}(\omega) = \underbrace{\frac{1}{C_\alpha} \omega^{-\alpha} \cos(\phi)}_{G_r} - j \underbrace{\frac{1}{C_\alpha} \omega^\alpha \sin(\phi)}_{H_r}, \quad (9)$$

where ϕ represents the phase shift given by the formula: $\phi = \alpha\pi/2$ [rad] or $\phi = 90\alpha$ [degree or $^\circ$]. As illustrated in Fig. S1 in the Supplementary Materials, the bounding values of α represent the discrete conventional elements: the resistor when $\alpha = 0$ and the capacitor when $\alpha = 1$). Additionally, from (9), it is clear that as α goes to 0, the imaginary part (H_r) of Z_C vanishes to 0 and hence the FOC characteristic becomes more like that a pure resistor, whereas as α approaches to 1, the real part (G_r) converges to 0 and hence, FOC operates as a pure capacitors. Furthermore, it has been demonstrated that the characteristics of FOC can be approximated using RC ladder structure [27]. Based on the above properties and in comparison to an integer order model where α is strictly fixed to an integer (0 or 1), the parameter α offers extra flexibility for a fractional-order paradigm. In connection with the apparent compliance modeling concept, FOC can be considered as a great candidate that might overcome the discrepancies stemming from integer-order limitation as follows:

- The proportionality constant C_α (pseudo-capacitance) is expressed in unit of [F.sec $^{1-\alpha}$] that makes, by its very nature, the conventional capacitance C , in the unit of [Farad], frequency-dependent, hence FOC has a physical foundation in representing the complex and frequency dependence of C_{app}
- Based on the order of the fractional differentiation factor α , the storage and the dissipation parts of the

resultant FOC's impedance can have different levels, as illustrated in Fig. S2, in the Supplementary Materials. Thus FOC might offer a key advantage in modeling complex system, that is the whole spectrum of dissipative and storage mechanisms may be included in a single parameter (the fractional differentiation order).

- The equivalent analog circuit of FOC can be viewed as infinity Voigt cells connected in parallel. Hence FOC might lead to a minimal representation of the mechanical properties of the arterial network by using only two parameters (α and C_α).

In biorheological research field, the imaginary, as well as the real part of Z_{FOC} , might represent the tissue damping (G_r) and tissue elastance (H_r), respectively:

$$\begin{cases} G_r(j\omega) = \frac{1}{C_\alpha \omega^\alpha} \cos(\alpha \frac{\pi}{2}) \\ H_r(j\omega) = -\frac{1}{C_\alpha \omega^\alpha} \sin(\alpha \frac{\pi}{2}) \end{cases} \quad (10)$$

The hysteresivity coefficient η_r (dimensionless) is defined as:

$$\eta_r = \frac{G_r}{H_r} = -\cot(\alpha \frac{\pi}{2}) \quad (11)$$

In general, these parameters are usually used to characterize the heterogeneity of the bio-tissue and are shown to be variable with pathology, as demonstrated for lung tissue for the respiratory system in [28].

B. Models

1) *Fractional order model of the dynamic Volume/Input-pressure relationship*: Recent researches have shown the key advantages of applying fractional calculus tools to describe correctly: 1) the viscoelasticity properties of the collagenous tissues in the arterial bed, 2) analyze the arterial blood flow [21], [22] and red blood cell (RBC) membrane mechanics [20] and, 3) modeling the heart valve cusp [29]. Bearing this in mind, in this part, we introduce the fractionalization of the dynamic relationship of the arterial blood volume and input-pressure. Based on the conservation mass, the arterial blood flow pumped from the heart to the arterial vascular bed (q_{in}) can be expressed as:

$$q_{in}(t) = q_{stored}(t) + q_{out}(t), \quad (12)$$

where q_{stored} is the blood stored in the arterial tree, and q_{out} corresponds to the flow out of the arterial system. As described in (3), q_{out} can be expressed as:

$$q_{out}(t) = \frac{1}{R_{app}} p_{in}(t). \quad (13)$$

Regarding q_{stored} , typically using the conventional definition, it can be determined as the rate of flow by taking the first derivative of the volume equation for the time, whereas, in consideration of the fractional properties of both RBC and the collagenous tissues forming the arterial bed, we allow the differentiation order of the blood volume for time to be real

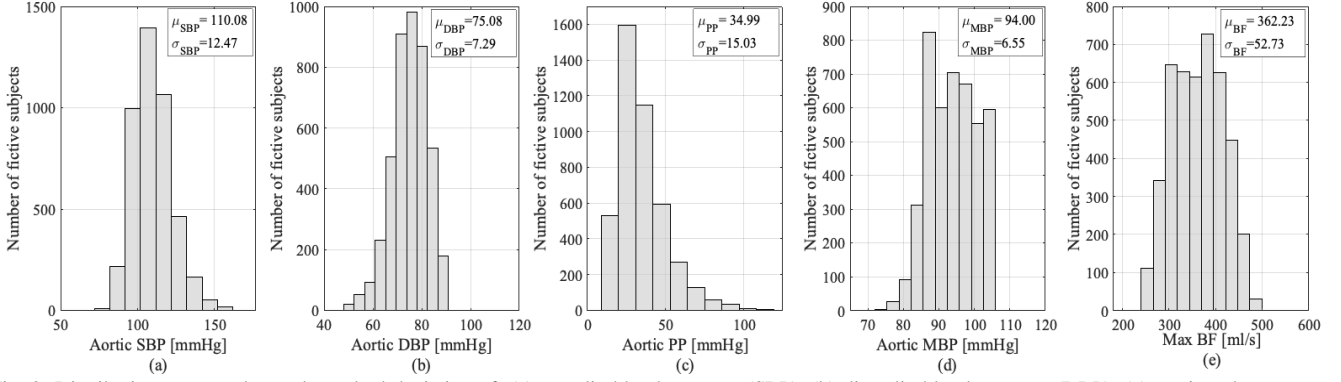


Fig. 2: Distribution, mean value and standard deviation of: (a) systolic blood pressure (SBP), (b) diastolic blood pressure (DBP), (c) aortic pulse pressure ($APP = SBP - DBP$), (d) mean blood pressure (MBP), and (e) the maximum of the blood flow (BF) at the level of ascending aorta for 4,374 virtual subject based in-silico database.

($\alpha \in [0 \ 1]$) and hence applying the fractional-order derivative to this differential equation.

$$q_{stored}(t) = D_t^\alpha V(t) = \frac{d^\alpha V(t)}{dt^\alpha}, \quad (14)$$

$$q_{stored}(t) = \underbrace{\frac{d^\alpha V(t)}{d^\alpha p_{in}(t)}}_{A_\alpha} \frac{d^\alpha p_{in}(t)}{dt^\alpha}, \quad (15)$$

where A_α is a fractional order proportionality constant that can be defined as a fractional order compliance expressed in the unit of $[1/\text{mmHg} \cdot \text{sec}^{1-\alpha}]$. Assuming null initial condition, the Laplace transform of (15) is given as:

$$Q_{stored} = A_\alpha s^\alpha P_{in}. \quad (16)$$

The conventional compliance in the unit of $[1/\text{mmHg}]$ that represents the complex and frequency-dependent apparent compliance can be written as follow:

$$C_c = A_\alpha s^{\alpha-1}. \quad (17)$$

Accordingly, by analogy to the electrical circuit, one may appropriately consider the fractional-order capacitor as a lumped parametric element to stand for the apparent arterial compliance. The voltage is equivalent to the arterial pressure; the electrical charges correspond to the blood volume and the electrical current as of the equivalent of the blood flow.

2) *Apparent compliance fractional-order Models*: In this part, we show the derivations of the proposed model based-structures for modeling the apparent arterial compliance. These structures scheme different combinations of FOC along with the conventional resistor and capacitor to display the complex and frequency-dependent behavior of the real dynamic compliance. Fig. 1 shows the proposed electrical analog structures of the proposed models.

Model A: It comprises only one single FOC. As detailed in the previous sections, the apparent compliance expressed in unit of $[1/\text{mmHg}]$ can be written as:

$$C_c^A = C_\alpha s^{\alpha-1}. \quad (18)$$

Model B: It comprises a resistor (R) and FOC connected in series. The apparent compliance expressed in the unit of

$[1/\text{mmHg}]$ can be written as:

$$C_c^B = \frac{C_\alpha s^{\alpha-1}}{1 + RC_\alpha s}. \quad (19)$$

Model C: It comprises an ideal capacitor (C_{stat}) accounting for the static compliance and FOC connected in series. The apparent compliance expressed in the unit of $[1/\text{mmHg}]$ can be written as:

$$C_c^C = \frac{C_\alpha C_{stat} s^\alpha}{C_\alpha s^\alpha + C_{stat}}. \quad (20)$$

Model D: It comprises a resistor (R), an ideal capacitor (C_{stat}) and FOC connected in series. The apparent compliance expressed in unit of $[1/\text{mmHg}]$ can be written as:

$$C_c^D = \frac{C_{stat} C_\alpha s^\alpha}{C_{stat} s + C_\alpha s^\alpha + RC_\alpha C_{stat} s^{\alpha+1}}. \quad (21)$$

Model E: It comprises a resistor (R_1) in parallel to a FOC and a resistor (R_2) connected in series. The apparent compliance expressed in unit of $[1/\text{mmHg}]$ can be written as:

$$C_c^E = \frac{1 + (R_1 + R_2) C_\alpha s^{\alpha-1}}{R_1 (1 + R_2 C_\alpha s^\alpha)}. \quad (22)$$

C. In-silico Virtual Population

Owing to a lack of real data to validate the proposed approaches, in this study, we utilize a virtual database of simulated pulse waves (PWs) [30]. The publicly available PW database¹ is considered a useful resource to evaluate the pre-clinical assessment of PWs analysis algorithms. The database encompasses mainly these arterial PWs: 1) flow velocity, 2) luminal area, 3) pressure and 4) photoplethysmogram pulse waves at different sites of the arterial network such as the ascending aorta, carotid artery, brachial artery, and radial arteries. The database represents samples of 4,374 virtual healthy adults aged from 25 to 75 years old, in ten-year increments (six age groups). For each age group, 729 virtual subjects based on pulse waves were created by varying specific cardiac and arterial parameters like the arterial stiffness and heart rate within normal ranges.

In this study, PWs at the level of ascending aorta have been investigated to evaluate our approaches. Fig. 2 shows

¹<https://peterhcharlton.github.io/pwdb/index.html>

a summary statistic of the aortic blood pressure parameter as well as the maximum blood flow at the level of the ascending aorta, for all virtual subjects. Additionally, we present a detailed statistic summary based on the group age and heart rate in Table SI in the supplementary material. This database presents physiological values with well-balanced distributions.

D. Identification Algorithm

The parameters of the proposed fractional-order models were estimated by a non-linear least square minimization routine, making use of the well-known MATLAB – R2019b, function *lsqnonlin*. This function is based on the trust-region reflective method [31]. The steps used to obtain the optimal estimates are outlined in Algorithm 1.

Algorithm 1 Parameter calibration of the apparent compliance models

- 1: Load the in-silico aortic blood pressure (P) and flow (Q)
- 2: Evaluate the Fast Fourier Transform (FFT) of both P and Q
- 3: Select the frequency range (Hz) $f \in [0 \ 12]$
- 4: Calculate the aortic input impedance Z_{in}
 - ▷ Using equation (1)
- 5: Calculate the in-silico apparent compliance C_{app}
 - ▷ Using equation (4)
- 6: Select the model to fit with the data
- 7: Include and Initialize the parameter to estimate Θ
 - % For instance for a single fractional-order capacitor based model (model A), $\Theta = \{C_\alpha, \alpha\}$
- 8:

$$RMSE = \sqrt{\frac{\sum_{i=1}^{N_s} \left(\frac{Re - \hat{Re}}{\max(Re)} \right)^2 + \left(\frac{Im - \hat{Im}}{Im} \right)^2}{N_s}}$$

$$\hat{\Theta} = \arg \min_{\Theta} RMSE$$

% Where N_s denoting the number of excited frequency points, Re and Im denoting the real and imaginary parts of the real C_{app} , and Im, evaluated in step (5), and \hat{Re} and \hat{Im} designate the real and imaginary parts of the model of C_{app} , respectively. $\hat{\Theta}$ denotes the estimates that minimize RMSE

In this study, we compare the performance of the proposed model with their corresponding integer-order version, where the fractional differentiation order α is equal to 1. Accordingly, the integer order version of model **A** will be equivalent to an ideal capacitor whose capacitance is a constant, which is not frequency-dependent, hence in our comparison, we exclude this case. Similarly, the integer-order version of model **C** leads to a series of two ideal capacitors, which is as well, equivalent to an ideal capacitor whose capacitance is constant. For the models, **B** and **D**, the integer-order version is equivalent to the analog Voigt cell model (an ideal

capacitor connected in series with a resistor). Conclusively, in this work, we compare our proposed methods to the Voigt cell model. On top of that, in order to show the role of fractional-order concept in reducing the complexity of such approach, we conduct an extra comparison with the well-known general apparent compliance-based model for viscoelastic material [32] which is expressed as:

$$C_c^F = C_{stat} \frac{\prod_{n=1}^N a_n(j\omega + b_n)}{\prod_{n=1}^N b_n(j\omega + a_n)}, \quad (23)$$

where a_n and b_n are imperial constants that can be convenient to fit any particular case. C_{stat} denoting the static compliance for the vessel. Goedhard et. all showed that this model could fit an experimental data with $N=4$. Hence in our comparison we choose $N=4$. We refer to the viscoelastic model and Voigt model as models **F** and **G**, respectively. Because the proposed models have a different number of parameter, to perform a fair comparison, the corrected Akaike Information Criterion (AIC_C) was evaluated:

$$AIC_C = -2\ln(RMSE) + \frac{2PN_s}{N_s - P - 1}, \quad (24)$$

where P is the number of parameters. Furthermore, the deviation of the model modulus from the in-silico apparent compliance modulus was calculated, using the following expression:

$$D_i [\%] = \left[\frac{|C_{c[i]}^{model}| - |C_{app[i]}|}{|C_{app[i]}|} \right]_{i=1..N_s} \times 100\%. \quad (25)$$

For ease of visualization of the various comparisons between the different models, for each virtual subject, we evaluated the mean of D [%] over the N_s harmonics, based on the following equation:

$$Deviation [\%] = \frac{\sum_{i=1}^{N_s} D_i [\%]}{N_s}. \quad (26)$$

III. RESULTS AND DISCUSSION

In this section, we first present a comparative evaluation between the proposed fractional-order model along with the integer-order ones. Afterward, we discuss the parameter estimates and their physiological insights.

A. Quantifying the models performances

The mean values of the goodness of fit criterion (NRMSE, Deviation(%) and AIC_C), after applying all the models, are depicted in Fig. 3, along with their box plots providing a visualization of summary statistics of this comparison. Additionally, we listed in Table SII, in the supplementary material, all the RMSE, Deviation and AIC_C mean values for each group of age and heart rate of the in-silico data. Fig. S3, in the Supplementary Materials represents a map of all the models with respect to the Deviation and the number of parameters to estimate (complexity). As for any modeling system, based on the fitting performance results, it is clear that there is a

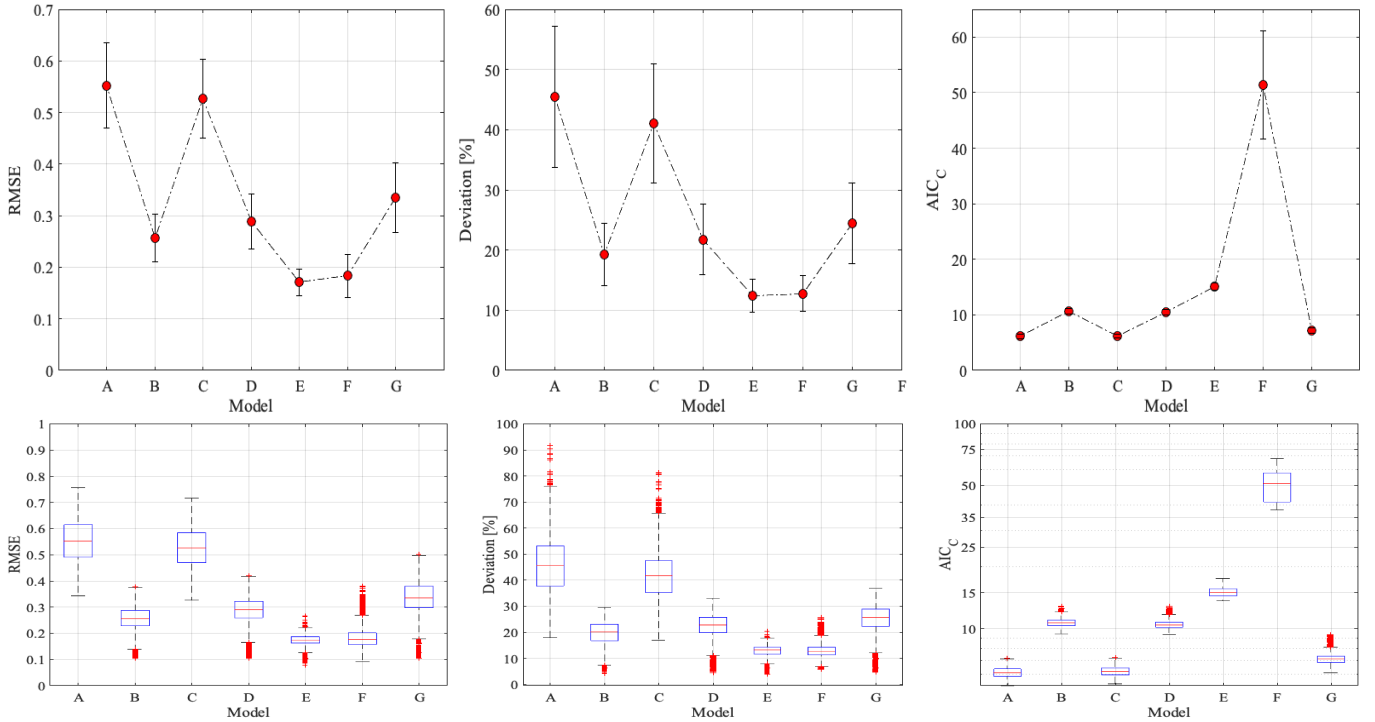


Fig. 3: Comparison of goodness of fit quantified as the mean values of RMSE , Deviation, and , AIC_c evaluated for both proposed models along with Viscoelastic and Voigt models for all the virtual subjects, and box plots providing a visualization of summary statistics of this comparison.

good compromise between the accuracy and complexity of the model. Among the five proposed fractional-order model, the single fractional-order capacitor-based, **Model A**, failed to produce the lowest RMSE and Deviation for any of the data sets; however, it represents the smallest (AIC_c). The fractional-order **Model E** and the integer-order **Model F** exhibit the lowest Deviation, as well as RMSE at the expense of the complexity that was reflected in the highest values of AIC_c. It is worth to mention that the fractional-order **Model E** comprises only four parameters and performed better than **Model F**, which possesses nine parameters. As illustrated in Fig.7, the best models that compromise between the complexity and the accuracy are **Model B**, **Model D**, and **Model G**. In terms of accuracy performance, among the latest models, the fractional-order **Model B** is performing the optimal. Conclusively, from the previous analysis, it is apparent that model system fractionalizing is enhancing the accuracy of the arterial compliance as well as reducing the complexity.

B. Statistical Analysis of the estimated parameters

1) *Model A*: Fig. 4 shows the distribution of the parameter estimates of Model A, after fitting the in-silico data of the arterial compliance. By observing the distribution of the fractional differentiation order, α , estimates, it is clear that this parameter is less than 1 for all the subjects. Its mean value is approximately 0.58 ± 0.008 . It is worth noting that in the estimation phase, for the parameter α , we have only constrained the lower bound to be zero; however, for the upper bound, it was unconstrained. Accordingly, this result indicates that the arterial system exhibits a viscoelastic behavior, not a purely elastic one. Indeed, the fact that $\alpha \neq 1$

implies that the FoC element incorporates both resistance and capacitance behaviors, as demonstrated mathematically in (10). This result further supports the concept of fractional-order behavior by the arterial system. In the proposed model, the fractional-order element combines both the resistance and the capacitance properties, which display the viscoelastic behavior of the arterial vessel. The contributions from both properties are controlled by the fractional differentiation order α , enabling a more flexible physiological description. As the fractional power approaches to 1, the capacitance part dominates and, hence the arterial system behaves like a pure elastic system.

2) *Model B*: Fig. 5 (a), (b), and (c) show the distribution of the parameter estimates of the Model B after fitting the in-silico data of the arterial compliance. By observing the distribution of α_B , it is clear that for all the subjects, this parameter

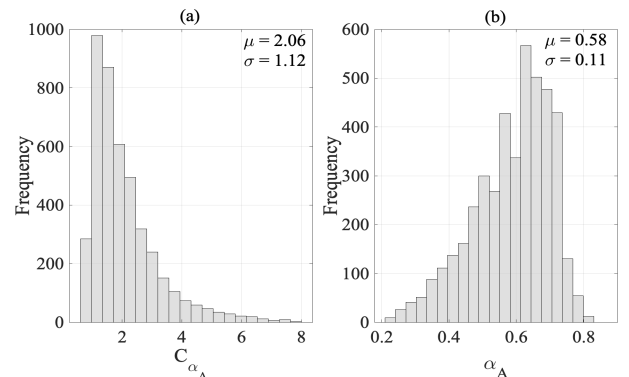


Fig. 4: Distribution, mean value and standard deviation of Model A parameter estimates: (a) the pseudo-capacitance C_{α_A} , and (b) the fractional differentiation order parameter α_A .

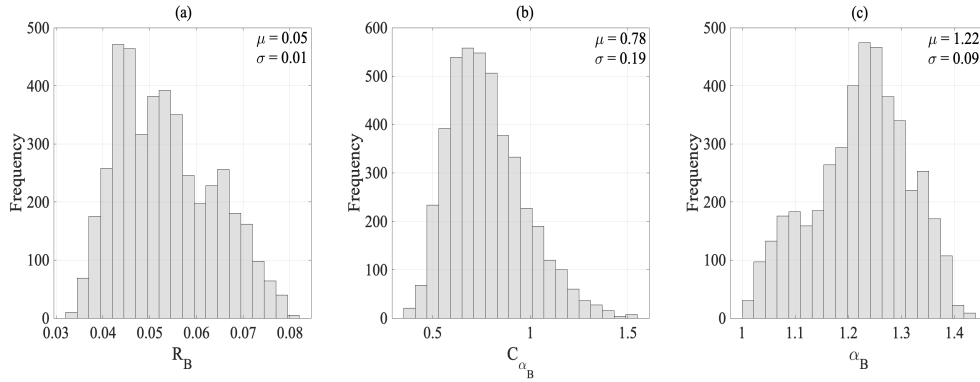


Fig. 5: Distribution, mean value and standard deviation of Model B parameter estimates: (a) the resistance R_B , (b) the pseudo-capacitance C_{α_B} , and (c) the fractional differentiation order parameter α_B .

is higher than 1 with a mean value of approximately equals to 1.22 ± 0.09 . Mathematically, as α exceeds 1, the real part of the fractional-order element impedance, G_r , becomes negative, and hence it has the characteristic of a negative resistor that supplies power. Having a negative resistance, in this case, comes as compensation for the added series resistance R_B . Besides, comparing to Model A, it is worthy to notice that the mean value of the pseudo-capacitance C_{α_B} was decreased to 0.78 ± 0.19 .

3) *Model C*: Fig. 6 (a) and (b) show the distribution of the parameter estimates of the Model C after fitting the in-silico data of the arterial compliance. In this model, the static capacitance has been chosen to be equal to the pseudo-capacitance. By observing the distribution of α_C , we can notice that this parameter is less than 1 for all the population with a mean value equal to 0.49 ± 0.10 . Comparing to Model A, the fractional factor has been decreased by approximately 0.1; however, the pseudo-capacitance was increased by 1. The decrease of α implies an increase of the resistive part of the FOC, as explained in the previous parts, which comes as to compensate for the increase in the overall capacitive part of the whole system model. In this model, the ideal capacitor is counting for static compliance, whereas the fractional-order one controls the arterial stiffness level. In other words, α might give a piece of information about the variation of the viscoelasticity of the arteries.

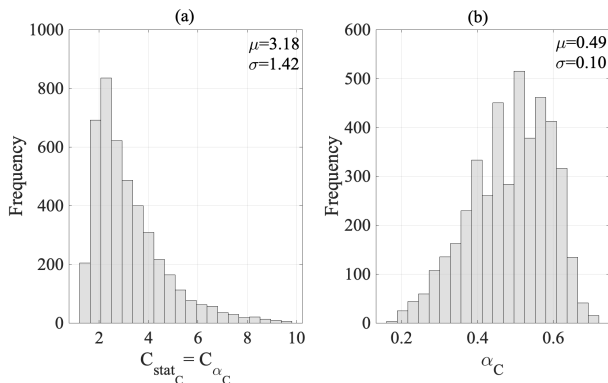


Fig. 6: Distribution, mean value and standard deviation of Model C parameter estimates: (a) the static capacitance $C_{stat_C} = C_{\alpha_C}$ which are equals, and (b) the fractional differentiation order parameter α_C .

4) *Model D*: Fig. 7 (a) and (b) show the distribution of the parameter estimates of the Model D after fitting the in-silico data of the arterial compliance. This model incorporates a static capacitor in series to FOC, along with a small resistor. Comparing to Model C, the addition of the small resistance causes α to go beyond 1 with a mean value approximately equal to 1.43 ± 0.14 . Besides, the mean value of static compliance and pseudo-capacitance decreases to 1.61 ± 0.50 . The addition of serial constant resistor and capacitor in this model is for the sake of account for the static viscosity and elasticity, respectively, while FOC depicts the ability of the arterial vessel to store blood dynamically.

5) *Model E*: Fig. 8 (a), (b), (c), and (d) show the distribution of the parameter estimates of the Model E after fitting the in-silico data of the arterial compliance. This model is similar to the equivalent analog circuit of Maxwell's mechanical element (series spring and dashpot in parallel with a dashpot), whereas instead of using an ideal capacitor to represent the spring, FOC has been employed. In terms of performance, Model E is the best. Similar to all the proposed model, $\alpha_D \in \mathbb{R}$ which demonstrate the fractional-order behavior of the apparent arterial compliance. By observing the distribution of R_{1E} R_{2E} , it is noticeable that these parameters are larger than R_B and R_D .

C. Relations between fractional-order parameters and central hemodynamic characteristics

Several research studies have observed that the changes in the determinants of the central blood pressure waveform, such as systolic blood pressure SBP, diastolic blood pressure DBP, and pulse pressure (APP), are strongly associated with cardiovascular diseases incidents. For instance, the augmentation of the SBP or APP is considered as a reflection marking the improper functioning of the cardiovascular system. In fact, stiffer arteries resulting from the arteriosclerosis disease causes increases in the SBP as well as arterial pulse wave velocity (PWV). PWV , such as carotid-to-femoral one (PWV_{cf}), are recognized as valuable surrogates of the arterial stiffness. In this part, we investigate whether the fractional differentiation order, α , and the hysteresivity coefficient, η_r , (defined by (11)) correlate with the central blood pressure determinants and the arterial pulse wave velocity (PWV_a) and (PWV_{cf}). In addition to the arterial pulse waves, the

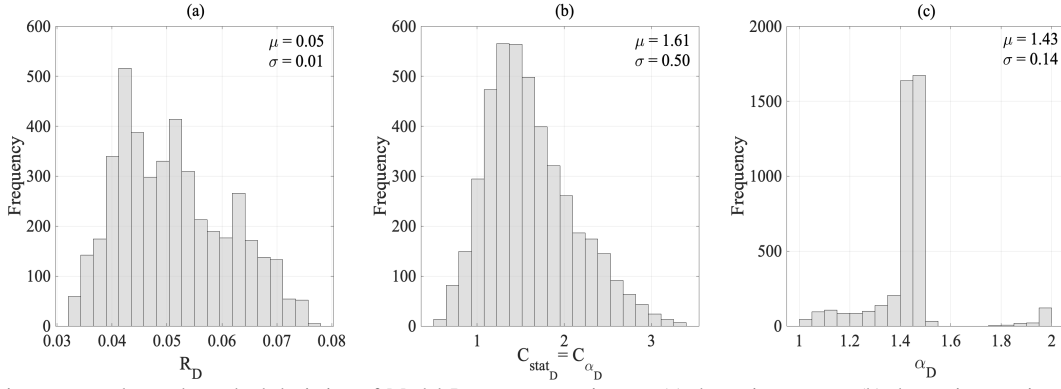


Fig. 7: Distribution, mean value and standard deviation of Model D parameter estimates: (a) the resistance R_D , (b) the static capacitance C_{stat_D} and the pseudo capacitance C_{α_D} which are equals, and (c) the fractional differentiation order parameter α_D .

used database provides both (PWV_a) and (PWV_{cf}) for each subject.

Accordingly, to evaluate the associations between the fractional-order parameters and the central hemodynamic determinants, for each model, we calculated the average value of α and η_r estimates over a fixed interval of the blood pressure determinant (SBP, DBP, and APP) that is equal to 5 [mmHg] and PWV that is equal to 0.5 [m/s]. Table I shows the correlation coefficients between α , and η_r and (SBP, DBP, APP, PWV_a and PWV_{cf}) (95% confidence interval). It is clear from these results that, for the majority of the models, the fractional-order parameters are strongly associated with the hemodynamic determinants. For instance, with regards to SBP, DBP, and APP, we notice that for all the proposed model, excepting for **Model D** the correlation coefficients with respect to η_r and α are larger or equal to 0.90. Regarding to the stiffness indexes, (PWV_a) and (PWV_{cf}), the coefficients correlation are approximately equal or larger than 0.85 for all the proposed model apart from **Model D**. Overall, the fractional-order parameter estimates of **Model B** present the best correlation coefficients. This result is in agreement with the goodness of the fit performance of this model. In fact, as analyzed in the previous parts, **Model B** provides a compromise between the accuracy and complexity of other proposed fractional-order models. In addition, although **Model A** is not very accurate in estimating the apparent compliance and not complicated, the

correlation coefficients between its parameter estimates and the hemodynamic determinant as well as the central PWVs are acceptable and reasonable.

Conclusively, our findings point out the potential interests of using FOC in the characterizing of arterial compliance. In addition, it demonstrates the viability of the fractional-order differentiation order to serve as a surrogate measure of the arterial stiffness or marker of cardiovascular diseases. Indeed, by assessing the fractional factor, α , it is easy to evaluate the hysteresivity coefficient η_r reflecting the ratio between two physiologically insightful parts: the tissue resistance and elastance.

D. Limitations

The fractional-order paradigm proposed in this work should be developed a little further before its generalization in the hemodynamic modeling context. In fact, It is worthy to note the limitations of this study. Firstly, in this work, due to the non-availability of real data, we used *in-silico* data. Although this database mimics the real physiological human states, and it is based on a validated one-dimensional numerical model of the arterial network, *in-vivo* investigations are required to validate and verify the reliability of the proposed models. The use of real data would considerably give more credibility to the new paradigm. Secondly, the estimation was based on only one cardiac cycle. Future work should derive

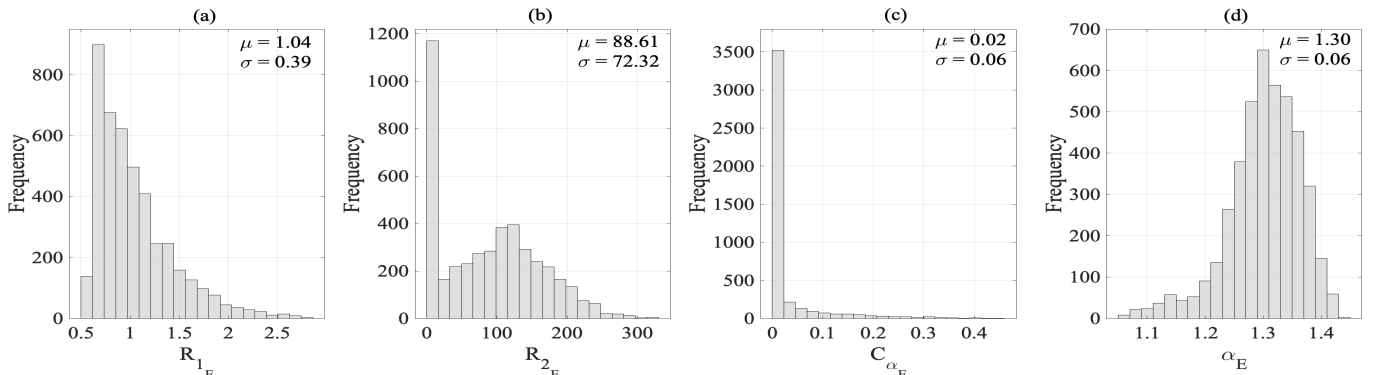


Fig. 8: Distribution, mean value and standard deviation of Model E parameter estimates: (a) the resistance R_{1_E} , (b) the resistance R_{2_E} , (c) the pseudo capacitance C_{α_E} , and (d) the fractional differentiation order parameter α_E .

TABLE I: Correlation coefficients between α and arterial systolic blood pressure (SBP), arterial diastolic blood pressure (DBP), arterial pulse pressure (APP), arterial pulse wave velocity (PWV_a) and carotid-femoral pulse wave velocity (PWV_{cf}) (95% confidence interval)

	SBP	DBP	APP	PWV_a	PWV_{cf}
α_A	0.96 (0.88 , 0.99)	-0.94 (-0.98 , -0.82)	0.92 (0.78 , 0.97)	0.85 (0.61 , 0.95)	0.87 (0.65 , 0.95)
η_{rA}	0.95 (0.85 , 0.98)	-0.94 (-0.98 , -0.83)	0.90 (0.74 , 0.97)	0.84 (0.58 , 0.94)	0.85 (0.62 , 0.95)
α_B	-0.99 (-1.00 , -0.96)	0.96 (0.88 , 0.99)	-0.97 (-0.99 , -0.91)	-0.98 (-0.99 , -0.93)	-0.97 (-0.99 , -0.92)
η_{rB}	-0.99 (-1.00 , -0.96)	0.96 (0.89 , 0.99)	-0.96 (-0.99 , -0.89)	-0.97 (-0.99 , -0.92)	-0.97 (-0.99 , -0.90)
α_C	0.97 (0.91 , 0.99)	-0.93 (-0.98 , -0.81)	0.94 (0.82 , 0.98)	0.88 (0.68 , 0.96)	0.89 (0.72 , 0.96)
η_{rC}	0.96 (0.87 , 0.99)	-0.93 (-0.98 , -0.81)	0.92 (0.77 , 0.97)	0.86 (0.64 , 0.95)	0.87 (0.66 , 0.96)
α_D	-0.92 (-0.97 , -0.78)	0.79 (0.48 , 0.92)	-0.89 (-0.96 , -0.71)	-0.79 (-0.92 , -0.48)	-0.68 (-0.88 , -0.28)
η_{rD}	0.35 (-0.20 , 0.73)	-0.65 (-0.87 , -0.22)	0.34 (-0.18 , 0.72)	0.25 (-0.28 , 0.66)	0.42 (-0.09 , 0.76)
α_E	-0.96 (-0.99 , -0.88)	0.95 (0.85 , 0.98)	-0.99 (-1.00 , -0.97)	-0.90 (-0.97 , -0.74)	-0.89 (-0.96 , -0.71)
η_{rE}	-0.96 (-0.99 , -0.89)	0.95 (0.86 , 0.98)	-0.99 (-1.00 -0.97)	-0.91 (-0.97 , -0.75)	-0.89 (-0.96 , -0.70)

metrics from multiple cycles. This will help to assess and take into account the inter-beat interval variability.

In addition, the presented approaches should be conducted in a range of different real physiological situations and show a good fitting for all the cases. It is straightforward to use FOC in the simple model representation proposed here, but there is no explicit agreement on the exact physiological relevance of the new parameter, the fractional differentiation order α or η_r . Although it is evident from mathematical equations that α value controls the viscosity as well as the elasticity levels, it would be of great potential for clinical application, to define ranges of the α value for normal and pathological physiological conditions. Finally, this study does not consider the noise effect on the pulse wave signals. In fact, several sources of noise can be allocated with the blood pressure signal, such as the movement artifacts, poor sensor contact, and optical interference, etc. Accordingly, considering the noise can impact the utility of the estimation of the fractional-order parameters. In the future, the robustness of the parameter estimates against the different sources of noise should be studied and analyzed. This is extremely important to especially assess arterial stiffness.

IV. CONCLUSION

The appearance of fractional-order behavior in the arterial system has been identified by many experimental studies of the viscoelasticity properties of the collagenous tissues in the arterial bed; the analyzes of the arterial blood flow and red blood cell membrane mechanics and the characterizing the heart valve cusp. This paper introduced a fractional-order modeling approach to assess the apparent arterial compliance. The models incorporate FOC along with ideal resistors and capacitors to display the dynamic relationship between the blood volume and aortic input pressure. The majority of proposed parametric models present reasonable fit performance with in-silico data. The results show that fractional-order model structures conveniently capture the capacity of the arterial system to store the blood. Besides, the fractional-order parameter estimates present good correlation coefficients with the central hemodynamic determinants, such

as the systolic and pulse blood pressure along with the central pulse wave velocity indexes. Thus, the fractional-order based approach of arterial compliance has a great potential to provide a new alternative in assessing the arterial stiffness. Future investigations will be directed toward integrating these models within a complete lumped-parameter model for the systemic circulation and study the effects of certain cardiovascular pathologies upon changes in the dynamic arterial compliance represented by the fractional-order capacitor.

ACKNOWLEDGMENT

Research reported in this publication was supported by King Abdullah University of Science and Technology (KAUST) Base Research Fund (BAS/1/162701-01). Additionally, the authors would like to thank Dr. Ali Haneef, associate consultant cardiac surgeon and co-chairman quality management at King Faisal Cardiac Center, King Abdulaziz Medical City, National Guard Health Affairs, in the Western Region, Jeddah, KSA and Dr. Nesrine T. Bahloul, medical intern at Department of Pediatrics, Sfax Medical School, Hedi Chaker Hospital, Sfax, Tunisia, for their assistance and valuable advices.

SUPPLEMENTARY MATERIALS

The Supplementary Information is described in more detail in the Supplementary Materials file, which includes the following Sections: (A) Fractional-order calculus section provides an overview about the Fractional-order derivative and its mathematical definitions; (B) Figures section represents Fig. S1: The schematic diagram for the resistor, capacitor, and fractional-order capacitor elements along with their $i-v$ characteristic relationships; Fig. S2: Modulus of (FOC impedance Z_C , left side), (the dissipation part Z_D) and (the storage part Z_S) for $C_\alpha = 1$; and Fig. S3: A map of all the models with respect to the Deviation and the number of parameters to estimate (complexity), and (C) Tables section presents three tables: Table SI: Mean value of systolic blood pressure (SBP), diastolic blood pressure (DBP), aortic pulse pressure (APP = SBP – DBP), mean blood pressure (MBP), and the maximum of the blood low (BF) at the level of

of ascending aorta for 4,374 virtual subject based in-silico database; Table SII: Mean values of the goodness of fit criterion (NRMSE, Deviation[%], and AIC_c of each age and heart rate based-group, and Table SIII: Mean value of the parameter estimates of the fractional-order models for each age and heart rate based-group.

REFERENCES

- [1] F. Liang and H. Liu, "A closed-loop lumped parameter computational model for human cardiovascular system," *JSME International Journal Series C Mechanical Systems, Machine Elements and Manufacturing*, vol. 48, no. 4, pp. 484–493, 2005.
- [2] T. Alderliesten, M. K. Konings, and W. J. Niessen, "Simulation of minimally invasive vascular interventions for training purposes," *Computer Aided Surgery*, vol. 9, no. 1-2, pp. 3–15, 2004.
- [3] E. Van Disseldorp, N. Pettersson, M. Rutten, F. Van De Vosse, M. van Sambeek, and R. Lopata, "Patient specific wall stress analysis and mechanical characterization of abdominal aortic aneurysms using 4d ultrasound," *European Journal of Vascular and Endovascular Surgery*, vol. 52, no. 5, pp. 635–642, 2016.
- [4] B. W. Beulen, N. Bijmens, G. G. Koutsouridis, P. J. Brands, M. C. Rutten, and F. N. van de Vosse, "Toward noninvasive blood pressure assessment in arteries by using ultrasound," *Ultrasound in medicine & biology*, vol. 37, no. 5, pp. 788–797, 2011.
- [5] W. Huberts, S. G. Heinen, N. Zonnebeld, D. A. van den Heuvel, J.-P. P. de Vries, J. H. Tordoir, D. R. Hose, T. Delhaas, and F. N. van de Vosse, "What is needed to make cardiovascular models suitable for clinical decision support? a viewpoint paper," *Journal of computational science*, vol. 24, pp. 68–84, 2018.
- [6] C. Leguy, E. Bosboom, H. Gelderblom, A. Hoeks, and F. Van De Vosse, "Estimation of distributed arterial mechanical properties using a wave propagation model in a reverse way," *Medical engineering & physics*, vol. 32, no. 9, pp. 957–967, 2010.
- [7] N. Stergiopoulos, J. Meister, and N. Westerhof, "Evaluation of methods for estimation of total arterial compliance," *American Journal of Physiology-Heart and Circulatory Physiology*, vol. 268, no. 4, pp. H1540–H1548, 1995.
- [8] N. Stergiopoulos, B. E. Westerhof, and N. Westerhof, "Total arterial inertance as the fourth element of the windkessel model," *American Journal of Physiology-Heart and Circulatory Physiology*, vol. 276, no. 1, pp. H81–H88, 1999.
- [9] C. M. Quick, D. S. Berger, and A. Noordergraaf, "Apparent arterial compliance," *American Journal of Physiology-Heart and Circulatory Physiology*, vol. 274, no. 4, pp. H1393–H1403, 1998.
- [10] C. M. Quick, D. S. Berger, D. A. Hettrick, and A. Noordergraaf, "True arterial system compliance estimated from apparent arterial compliance," *Annals of biomedical engineering*, vol. 28, no. 3, pp. 291–301, 2000.
- [11] D. Craiem and R. Armentano, "The new apparent compliance concept as a simple lumped model," *Cardiovascular Engineering: An International Journal*, vol. 3, no. 2, pp. 81–83, 2003.
- [12] R. Burattini and S. Natalucci, "Complex and frequency-dependent compliance of viscoelastic windkessel resolves contradictions in elastic windkessels," *Medical engineering & physics*, vol. 20, no. 7, pp. 502–514, 1998.
- [13] R. Visaria, *Modeling of cardiovascular system, pulmonary mechanics and gas exchange*. The University of Utah, 2005.
- [14] C. M. Ionescu, J. T. Machado, and R. De Keyser, "Modeling of the lung impedance using a fractional-order ladder network with constant phase elements," *IEEE Transactions on biomedical circuits and systems*, vol. 5, no. 1, pp. 83–89, 2010.
- [15] Y. Kobayashi, A. Kato, H. Watanabe, T. Hoshi, K. Kawamura, and M. G. Fujie, "Modeling of viscoelastic and nonlinear material properties of liver tissue using fractional calculations," *Journal of Biomechanical Science and Engineering*, vol. 7, no. 2, pp. 177–187, 2012.
- [16] R. L. Magin, *Fractional calculus in bioengineering*. Begell House Redding, 2006.
- [17] A. Jaishankar and G. H. McKinley, "Power-law rheology in the bulk and at the interface: quasi-properties and fractional constitutive equations," *Proceedings of the Royal Society A: Mathematical, Physical and Engineering Sciences*, vol. 469, no. 2149, p. 20120284, 2013.
- [18] D. Craiem and R. L. Armentano, "A fractional derivative model to describe arterial viscoelasticity," *Biorheology*, vol. 44, no. 4, pp. 251–263, 2007.
- [19] D. Craiem, F. J. Rojo, J. M. Atienza, R. L. Armentano, and G. V. Guinea, "Fractional-order viscoelasticity applied to describe uniaxial stress relaxation of human arteries," *Physics in Medicine & Biology*, vol. 53, no. 17, p. 4543, 2008.
- [20] D. Craiem and R. L. Magin, "Fractional order models of viscoelasticity as an alternative in the analysis of red blood cell (rbc) membrane mechanics," *Physical biology*, vol. 7, no. 1, p. 013001, 2010.
- [21] P. Perdikaris and G. E. Karniadakis, "Fractional-order viscoelasticity in one-dimensional blood flow models," *Annals of biomedical engineering*, vol. 42, no. 5, pp. 1012–1023, 2014.
- [22] J. P. Zerpa, A. Canelas, B. Sensale, D. B. Santana, and R. Armentano, "Modeling the arterial wall mechanics using a novel high-order viscoelastic fractional element," *Applied Mathematical Modelling*, vol. 39, no. 16, pp. 4767–4780, 2015.
- [23] M. A. Bahloul and T. M. Laleg-Kirati, "Three-element fractional-order viscoelastic arterial windkessel model," in *2018 40th Annual International Conference of the IEEE Engineering in Medicine and Biology Society (EMBC)*. IEEE, 2018, pp. 5261–5266.
- [24] —, "Arterial viscoelastic model using lumped parameter circuit with fractional-order capacitor," in *2018 IEEE 61st International Midwest Symposium on Circuits and Systems (MWSCAS)*. IEEE, 2018, pp. 53–56.
- [25] M. A. Bahloul and T.-M. L. Kirati, "Fractional order models of arterial windkessel as an alternative in the analysis of the left ventricular afterload," *arXiv preprint arXiv:1908.05239*, 2019.
- [26] M. Nakagawa and K. Sorimachi, "Basic characteristics of a fractance device," *IEICE Transactions on Fundamentals of Electronics, Communications and Computer Sciences*, vol. 75, no. 12, pp. 1814–1819, 1992.
- [27] G. Tsirimokou, "A systematic procedure for deriving rc networks of fractional-order elements emulators using matlab," *AEU-International Journal of Electronics and Communications*, vol. 78, pp. 7–14, 2017.
- [28] C. M. Ionescu, *The human respiratory system: an analysis of the interplay between anatomy, structure, breathing and fractal dynamics*. Springer Science & Business Media, 2013.
- [29] T. C. Doehring, A. D. Freed, E. O. Carew, and I. Vesely, "Fractional order viscoelasticity of the aortic valve cusp: an alternative to quasi-linear viscoelasticity," *Journal of biomechanical engineering*, vol. 127, no. 4, pp. 700–708, 2005.
- [30] P. Charlton, J. Mariscal Harana, S. Vennin, Y. Li, P. Chowienczyk, and J. Alastruey, "Modelling arterial pulse waves in healthy ageing: a database for in silico evaluation of haemodynamics and pulse wave indices," *American Journal of Physiology-Heart and Circulatory Physiology*, 2019.
- [31] T. F. Coleman and Y. Li, "An interior trust region approach for nonlinear minimization subject to bounds," *SIAM Journal on optimization*, vol. 6, no. 2, pp. 418–445, 1996.
- [32] W. Goedhard and A. Knoop, "A model of the arterial wall," *Journal of biomechanics*, vol. 6, no. 3, pp. 281–288, 1973.